PNAS RESEARCH ARTICLE | DEVELOPMENTAL BIOLOGY OPEN ACCESS

Injury-induced MAPK activation triggers body axis formation in *Hydra* by default Wnt signaling

Anja Tursch[a], Natascha Bartsch[a,b], Moritz Mercker[c], Jana Schlüter[d], Mark Lommel[a,e], Anna Marciniak-Czochra[c], Suat Özbek[a], and Thomas W. Holstein[a,1]

Edited by Roel Nusse, School of Medicine, Stanford University, Stanford, CA; received March 8, 2022; accepted July 12, 2022

***Hydra*'s almost unlimited regenerative potential is based on Wnt signaling, but so far it is unknown how the injury stimulus is transmitted to discrete patterning fates in head and foot regenerates. We previously identified mitogen-activated protein kinases (MAPKs) among the earliest injury response molecules in *Hydra* head regeneration. Here, we show that three MAPKs—p38, c-Jun N-terminal kinases (JNKs), and extracellular signal-regulated kinases (ERKs)—are essential to initiate regeneration in *Hydra*, independent of the wound position. Their activation occurs in response to any injury and requires calcium and reactive oxygen species (ROS) signaling. Phosphorylated MAPKs hereby exhibit cross talk with mutual antagonism between the ERK pathway and stress-induced MAPKs, orchestrating a balance between cell survival and apoptosis. Importantly, *Wnt3* and *Wnt9/10c*, which are induced by MAPK signaling, can partially rescue regeneration in tissues treated with MAPK inhibitors. Also, foot regenerates can be reverted to form head tissue by a pharmacological increase of β-catenin signaling or the application of recombinant Wnts. We propose a model in which a β-catenin-based stable gradient of head-forming capacity along the primary body axis, by differentially integrating an indiscriminate injury response, determines the fate of the regenerating tissue. Hereby, Wnt signaling acquires sustained activation in the head regenerate, while it is transient in the presumptive foot tissue. Given the high level of evolutionary conservation of MAPKs and Wnts, we assume that this mechanism is deeply embedded in our genome.**

regeneration | injury response | MAPK signaling | axis formation | Wnt/beta-catenin

Significance

Wnt signaling pathways are found exclusively in animal systems. They are of crucial importance for development, cell differentiation, and tumorigenesis. Wnt signaling pathways are also instrumental for regenerative processes from *Hydra* to humans. Here we show that Wnt signaling is activated by default after an injury as a consequence of generic mitogen-activated protein kinase phosphorylation to drive tissues into a regeneration-competent state. Positional specification at later stages is achieved by a tissue-dependent sensitivity to the generic wound signals, which either allows or prevents the establishment of a persisting Wnt/β-catenin feedback loop and axis formation.

The ability to regenerate varies widely across species. Basal animals, like cnidarians and planarians, can regenerate their whole body, while most vertebrates and mammals have only limited regeneration capacity (1, 2). There are some notable examples for the regeneration of entire body parts in vertebrates, e.g., limb regeneration in salamanders (3, 4). In all cases, following an injury, regeneration starts with wound healing, after which cells at the site of injury begin to proliferate and form a blastema, from which the missing structures are repatterned (5, 6). Intriguingly, embryonal signaling pathways and gene regulatory networks (GRNs) are often reactivated during this injury-triggered regeneration process (7–13). Although several studies have advanced our knowledge about how the initial injury activates pattern formation, resulting in the faithful replacement of lost structures (14–17), this important question is still not fully understood. Thus, a deep understanding of the molecular interactions between wounding and pattern formation may shed light not only on the field of regenerative and developmental biology but likewise on the formation of solid tumors, in which mechanisms acting during regeneration may have been coopted (6).

Here, we investigated the linkage between injury signals and pattern formation in the freshwater polyp *Hydra*, in which the phenomenon of regeneration was initially discovered when Trembley (in 1744) cut polyps into two halves (18). Even today, we do not understand why, at the cutting interface and virtually from the same gastric tissue, in the lower half of a polyp a head and in the upper half a foot are regenerated (18–20). At the molecular level, one of the best-established facts is our initial finding that Wnt/β-catenin signaling is a key player in *Hydra* head regeneration (21–27), which was also confirmed in a number of further studies (25, 28–31). However, recent works have shown that a transient up-regulation of β-catenin also occurs during foot regeneration in *Hydra* (32). This finding calls into question an exclusive role in position-specific patterning but opens up the intriguing perspective that differential Wnt codes might instruct the discrete patterning processes in head and foot regenerates.

There is strong evidence that the injury signal contains molecular cues essential for *Hydra*'s regeneration. When cutting is replaced by a careful ligature with a hair, it is possible to remove the polyp's head without injury (33, 34). Such animals failed to

Author affiliations: [a]Molecular Evolution & Genomics, Centre for Organismal Studies, Heidelberg University, 69120 Heidelberg, Germany; [b]Department of Biological Sciences, Bergen University, 5020 Bergen, Norway; [c]Institute of Applied Mathematics, Heidelberg University, 69120 Heidelberg, Germany; [d]Department of Neurobiology, Interdisciplinary Center of Neurosciences, Heidelberg University, 69120 Heidelberg, Germany; and [e]Department of Microbiology, Saarland University, 66123 Saarbrücken, Germany

Author contributions: A.T., S.Ö., and T.W.H. designed research; A.T., N.B., J.S., and M.L. performed research; J.S. and T.W.H. contributed new reagents/analytic tools; A.T., N.B., M.M., M.L., A.M.-C., S.Ö., and T.W.H. analyzed data; and A.T., S.Ö., and T.W.H. wrote the paper.

The authors declare no competing interest.

This article is a PNAS Direct Submission.

[1]To whom correspondence may be addressed. Email: thomas.holstein@cos.uni-heidelberg.de.

This article contains supporting information online at http://www.pnas.org/lookup/suppl/doi:10.1073/pnas.2204122119/-/DCSupplemental.

Published August 22, 2022.

regenerate a new head, indicating that signals released upon injury are essential to initiate this process. Studies with a regeneration-deficient strain (*Hydra magnipapillata* reg-16) showed that after repeated wounding of the tissue, the animals were able to regenerate again (35, 36). Remarkably, a similar effect was obtained when decapitated reg-16 polyps were exposed to recombinant Wnt3 (27). This indicates a linkage between injury and *Wnt* expression during *Hydra* regeneration, although it is unclear which signals activate Wnt signaling.

Recently, we identified several mitogen-activated protein kinases (MAPKs) that showed a sharp increase in phosphorylation upon wounding and are thus assumed to play an important role during the injury response (37). We therefore decided to investigate the roles of extracellular signal-regulated kinase (ERK), p38 MAPK (p38), and c-Jun N-terminal kinase (JNK) in *Hydra* injury and regeneration. Among the MAPKs acting in *Hydra* regeneration, previous studies have identified mainly ERK as implicated (38–41). Here a large body of work from the Galliot laboratory (40, 42, 43) has focused on the ERK targets RSK and CREB. RSK is a phosphorylation target of ERK, and RSK's target CREB has been shown to be also phosphorylated downstream of MEK activity in head regenerates (42) and in proapoptotic cells of head regenerates (40). This work demonstrated that MEK activity is required for head regeneration (42). However, it is hitherto unknown whether and how MAPK pathways are linked with Wnt-regulated patterning processes. In planarian regeneration, it was shown that ERK and Wnt/β-catenin signaling pathways interact in a position-specific manner (44) and JNK is involved in control of apoptosis and mitosis during regeneration (45). In *Hydra,* apoptotic interstitial cells are claimed to release Wnt3 at the wound sites of head, but not foot, regenerates via a yet-unknown mechanism (29).

Here, we show that bisecting the animal triggers a cascade of wounding signals, including Ca^{2+}, reactive oxygen species (ROS), and MAPK signaling, that induces apoptosis and finally *Wnt* expression at both wound sites. Recombinant Wnt3 or Wnt9/10 was able to rescue impaired MAPK signaling, suggesting that the MAPK-dependent activation of Wnts is part of a generic wound response that leads to pattern formation in the regenerate. Our data also demonstrate that the injury signal can trigger the patterning system through activation of *Wnt* genes by MAPK signaling-responsive Activating Transcription Factors (ATFs). The capacity for head formation by injury-activated *Wnt* genes strongly depends on the signaling context of the injured tissue. A pharmacological increase of β-catenin activity or treatment with recombinant Wnts induces head formation in a tissue that normally would regenerate a foot, indicating that a high level of β-catenin activity favors head regeneration. We propose a model in which β-catenin and the basal oral-aboral source density gradient of *Hydra*'s body, after an initial phase of indiscriminate injury response, determine the fate of the regenerating tissue.

Results

MAPK activation is a general response to injury in *Hydra* and required for regeneration. Our previous phosphoproteome analysis revealed rapid changes in protein phosphorylation and dephosphorylation in response to injury (37). Among other factors, several MAPKs showed rapid phosphopeptide enrichment upon wounding, indicating an important role for the injury response. Because of their sharp increase in phosphorylation, we selected ERK, p38, and JNK for biochemical analysis to evaluate their phosphorylation dynamics upon injury. Moreover, to test whether MAPK activation is directly dependent on the wound signal, we took advantage of previous observations that tissue separation by simple ligation leads to a massive decrease in regenerative capacity (33, 34), most likely due to the absence of an injury stimulus, by preserving epithelial integrity, as evidenced by propidium-iodide staining (Fig. 1*A*).

First, we analyzed how the phosphorylated (and thus activated) levels of ERK, p38, and JNK changed in response to injury and regeneration of head and foot tissue. We used commercially available antibodies specific for the phosphorylated epitopes in the given MAPKs that were fully conserved in the respective *Hydra* orthologs (*SI Appendix*, Fig. S1), as also evidenced by the matching molecular masses of the detected western blot bands (*SI Appendix*, Fig. S2*A*). We bisected polyps and prepared tissue lysates from entire polyp fragments at various time points after injury. All MAPKs tested showed a similar increase in phosphorylation within the first minutes postinjury (pi), with a maximum at 30 to 60 min pi, while total protein levels remained unaffected (Fig. 1 *B* and *C* and *SI Appendix*, Fig. S2 *B* and *C*). Interestingly, while the phosphorylated JNK (pJNK) and phosphorylated p38 (pp38) levels started to decrease after 60 min, phosphorylated ERK (pERK) was still detectable until 6 h pi (*SI Appendix*, Fig. S2*B*). Of note, the increase of activated MAPKs was less pronounced in tied animals, indicating that phosphorylation occurs in response to the wound stimulus (Fig. 1*B*). Moreover, the increase of pERK, pp38, and pJNK was similar in regenerating head and foot pieces, suggesting that the injury-induced activation occurs independent of wound position (Fig. 1*C*).

Next, we used immunofluorescence (IF) analysis to determine the localization of pERK, pJNK, and pp38 relative to the wound site (Fig. 1 *D* and *E* and *SI Appendix*, Fig. S3 *A–D*). MAPKs localized to epithelial cells, where pERK and pJNK showed a cytoplasmic and pp38 showed a nuclear distribution (Fig. 1*D* and *SI Appendix*, Fig. S3 *A–C*). To our surprise, activated MAPKs were not restricted to the wound site but instead dispersed in a gradient emanating from the wound edge (Fig. 1 *E*, cut). This occurred at a similar level in head and foot regenerates, indicating a position-independent response to injury. We also found a similarly strong induction of MAPK activity when making an incision in the body—which is a nonregenerative injury—indicating MAPK activation as a general response to tissue injury (Fig. 1 *E*, incision). Interestingly, in agreement with our western blot data, the IF signals of pERK, pp38, and pJNK in tied polyps were strongly diminished compared to those of animals cut with a scalpel (Fig. 1 *E*, tied).

We next tested if MAPKs that were activated upon injury are required for head and foot regeneration using inhibitors specific for ERK (U1026), p38 (SB203580), and JNK (SP600125). U0126 is a direct noncompetitive inhibitor of the MAPK family members MEK-1 and MEK-2, which are the upstream kinases of ERK (46). Thus, the use of U0126 prevents the phosphorylation of ERK, and because of its specificity, we refer to it as ERK inhibitor for simplicity. In contrast, the inhibitors SB203580 and SP600126 directly bind to the Adenosine triphosphate (ATP) binding pocket of p38 and JNK, respectively, in a competitive manner, thereby prohibiting the phosphorylation of p38's and JNK's downstream targets but not phosphorylation of the kinases themselves (42, 47, 48).

To test the effect of these inhibitors on head regeneration, heads were removed by cutting at a 70% distance from the aboral end, and the fraction of properly regenerated heads at 72 h postamputation (hpa) was determined (Fig. 1 *F* and *G*). The majority of control regenerates (92%) exhibited a fully regenerated head with a hypostome and a ring of tentacles. By contrast, all regenerates treated with MAPK inhibitors showed

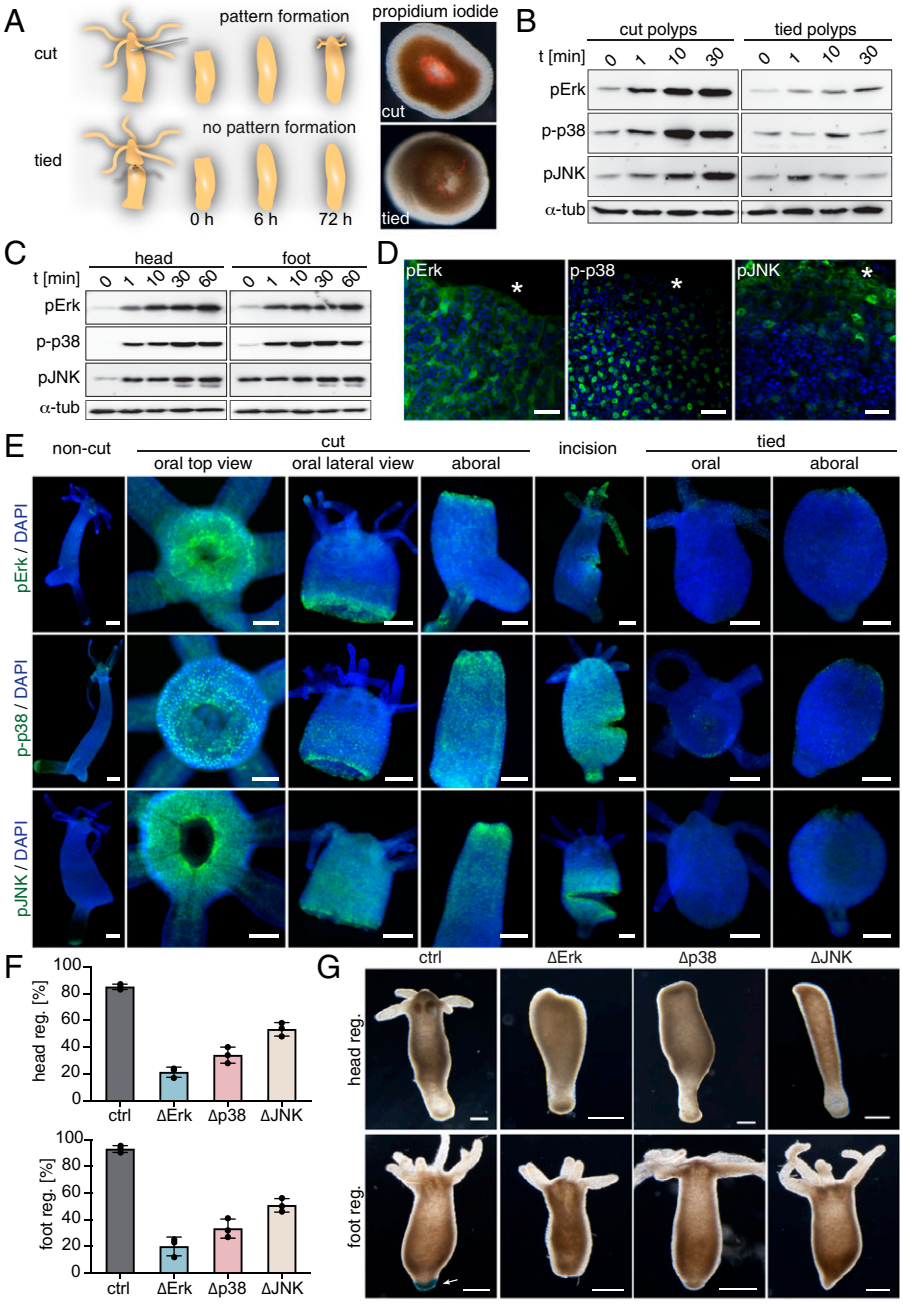

Fig. 1. MAPK activation is injury dependent and required for the initiation of regeneration. (*A*) Experimental scheme showing decapitation by cutting (wounding) or careful ligation (without wounding). Ligated animals cannot regenerate properly due to preserved epithelial integrity, as indicated by propidium staining 30 min after injury/ligation. (*B*) Phosphorylation of MAPKs is reduced in ligated polyps. Regenerates from cut or tied animals were analyzed by western blot after the indicated time points using phospho-specific MAPK antibodies and α-tubulin specific antibody (α-tub as control (*Materials and Methods*). (*C*) Equal activation of MAPKs in head and foot regenerates as detected by phospho-specific antibodies, as in *B*. (*D* and *E*) Confocal images of regenerating and injured polyps with phospho-specific antibodies for ERK, p38, and JNK 30 min after amputation/injury/ligation. (*D*) Lateral view on the wound site (asterisk) of regenerating polyps postamputation shows a cytoplasmic distribution for activated ERK and JNK, while p38 localizes to nuclei. Scale bar: 50 μm. (*E*) IF analysis of MAPK activation at the injury site in lateral views 30 min after injury; the column with the oral top view additionally shows the direct view of the wound site. Phospho-specific antibodies revealed gradient-like activation MAPKs peaking at the site of amputation or incision as indicated. Note that the tissue completely lacked MAPK activation in tied polyps. Nuclei were stained using DAPI (blue). Scale bars: 250 μm each. (*F* and *G*) Inhibition of MAPK activity prevents head and foot regeneration. Polyps were bisected and the proximal and distal parts were allowed to regenerate in the presence of inhibitors specific for ERK, p38, and JNK. Foot regenerates were evaluated by peroxidase staining, as shown in *G*. Error bars indicate the mean of three independent experiments with SD. Head regeneration (head reg.): *n* (control [ctrl]) = 108, *n* (ΔERK) = 61, *n* (Δp38) = 58, *n* (ΔJNK) = 72. Foot regeneration (foot reg.): *n* = 45 per condition. (*G*) Representative pictures from the experiment described in *F*. The white arrow indicates the basal disk stained with peroxidase. Scale bars: 500 μm.

regeneration deficiencies. Although the wound was closed, head regeneration was significantly impaired in animals treated with ERK, p38, and JNK inhibitors. To test the function of MAPKs during foot regeneration, we dissected animals at 30% of the body length and used the peroxidase assay to visualize differentiated foot tissue (49). In untreated controls, 98% of *Hydra* were positive for peroxidase activity at the aboral end at 72 hpa, which indicates full regeneration of the basal disk. In contrast, the majority of inhibitor-treated animals did not show peroxidase activity, although wound healing was normal, as in the head regenerates (Fig. 1*G*). The inhibitory effect of U0126 on head regeneration was shown to be dose dependent (10 to 20 μM) (42), and our data indicate that a higher dose (25 μM) is required to inhibit foot regeneration (*Discussion*). Taken together, these findings demonstrate that MAPK phosphorylation occurs as a general response to an injury stimulus in a position-independent manner and is essential for the onset of regeneration in *Hydra*.

p38 and JNK Activation Depends on ROS Signaling. Given the importance of MAPK signaling in regeneration, we next set out to determine how MAPKs are activated in response to injury. We considered ROS because recent work in zebrafish and *Drosophila* showed the importance of ROS for regeneration and cell proliferation, probably by either activating or modulating different signaling pathways such as JNK or Hedgehog signaling (50, 51). To test whether ROS is produced at the site of injury, animals were incubated with CellRox prior to amputation (*SI Appendix*, Fig. S4). Indeed, bisected animals incubated with this dye showed a fluorescent signal at the wounded edge, indicating ROS production (*SI Appendix*, Fig. S4*A*). Incubation with the oxidizing reagent hydrogen peroxide (H_2O_2) increased the signal intensity at the injury site. Conversely, the signal was abolished when animals were incubated with reduced glutathione (GSH) or bisected without injury by tying (*SI Appendix*, Fig. S4). To test whether the redox state has an impact on the

activation levels of MAPKs, animals were incubated in *Hydra* medium (HM) or in HM supplemented with either H_2O_2 or GSH to produce an oxidizing or reducing environment, respectively. The exposure to H_2O_2 resulted in elevated activation levels for all MAPKs tested (Fig. 2*A*). Incubation with reduced GSH resulted in decreased activation of p38 and JNK after wounding, while the effect was less pronounced for pERK (Fig. 2*A*). These findings were further supported by IF analyses using the same experimental setup. In the presence of H_2O_2, the signal intensity of activated ERK, p38, and JNK was increased and their distribution along the tissue was expanded (Fig. 2*B* and *SI Appendix*, Fig. S4*C*). Treatment with GSH reduced levels of p38 and JNK activation throughout the tissue, while effects on pERK were not evident (Fig. 2*B*), which is in line with our western blot analysis.

We next tested if manipulating the redox state has an effect on regeneration by incubating bisected *Hydra* in the presence of either H_2O_2 or GSH (Fig. 2 *C* and *D*). Animals regenerated normally under oxidative conditions. By contrast, on average, 65% of *Hydra* head regenerates and 60% of *Hydra* foot regenerates did not proceed under reducing conditions (Fig. 2 *C* and *D*). These data support a model according to which the activation of MAPKs and the initiation of regeneration are stimulated by ROS production after injury.

MAPK Activation Depends on Ca^{2+} Signaling. Calcium signaling is one of the fastest transduction pathways across cells and is involved in many processes, including wound closure and regeneration (52, 53). Given the fast kinetics of MAPK phosphorylation in response to wounding (Fig. 1*B*), we hypothesized that Ca^{2+} signaling is responsible for the gradient-like transmission of the injury signal. To test this, we performed live cell imaging of transgenic strains in which polyps express a genetically encoded Ca^{2+} indicator (GCaMP) in ectodermal or endodermal epithelial muscle cells. This allowed us to analyze the Ca^{2+} dynamics in intact and sectioned animals by measuring the fluorescence signal over time (Fig. 3 *A* and *B*). When intact animals were stimulated to contract by a short poke with tweezers, but without injury, we found a slight and transient Ca^{2+} release in both germ layers (Movies S1–S9). In contrast, the amplitude of the fluorescence signal was increased threefold in cut animals in both germ layers and at both section sites. Also, the duration of the increase lasted significantly longer in cut animals than in intact animals, with the exception of the oral section site in the endodermal strain. This tendency was, although less pronounced, also observable in polyps cut in calcium-free medium, indicating that the calcium signal is generated in part by intracellular release (*SI Appendix*, Fig. S5*A*).

To test whether intracellular Ca^{2+} levels affect MAPK activation, we either increased the intracellular calcium levels by treating polyps with the Ca^{2+} ionophore A23187 or reduced them by incubation with the Ca^{2+} chelator 1,2-bis(o-aminophenoxy)ethane-N,N,N′,N′-tetraacetic acid (BAPTA). *SI Appendix*, Fig. S5*B* shows that in bisected animals, exposure to BAPTA resulted in reduced and delayed Ca^{2+} release upon amputation, whereas treatment with A23187 resulted in elevated levels for more than 4 min (Movies S10 and S11). When polyps were exposed to BAPTA after injury, they showed decreased phosphorylation levels of p38, ERK, and JNK in both western blot analysis and IF staining (Fig. 3 *C* and *D*). Conversely, treatment with A23187 led to an increase of MAPK activation (Fig. 3*C*). Interestingly, exposure to A23187 did not necessarily result in enhanced staining signals at the wounded edge but rather resulted in uniform distribution of activated MAPKs along the entire body column (Fig. 3*D*).

Because MAPK inhibition abrogated the initiation of regeneration, we tested whether reduction of Ca^{2+} levels and thus MAPK phosphorylation also affects the regenerative capacity in *Hydra*. We found that reduction of Ca^{2+} levels by BAPTA treatment resulted in a decrease of head regeneration capacity to 60% during the first 3 h after wounding and cotreatment with ethylene glycol-bis(β-aminoethyl ether)-N,N,N′,N′-tetraacetic acid) (EGTA) caused a further reduction to 32% (Fig. 3 *E* and *F*). Likewise, regeneration of the foot decreased to 65% in the presence of BAPTA and to 45% when a combination of BAPTA and EGTA was used. Taken together, injury promotes the release of both ROS and Ca^{2+} that in turn acts positively on the activation of MAPK-induced regeneration. We therefore next searched for the putative targets of MAPK activation.

Wnt Expression Is Generically Initiated upon Injury. Wnt signaling is an essential pathway for head regeneration and

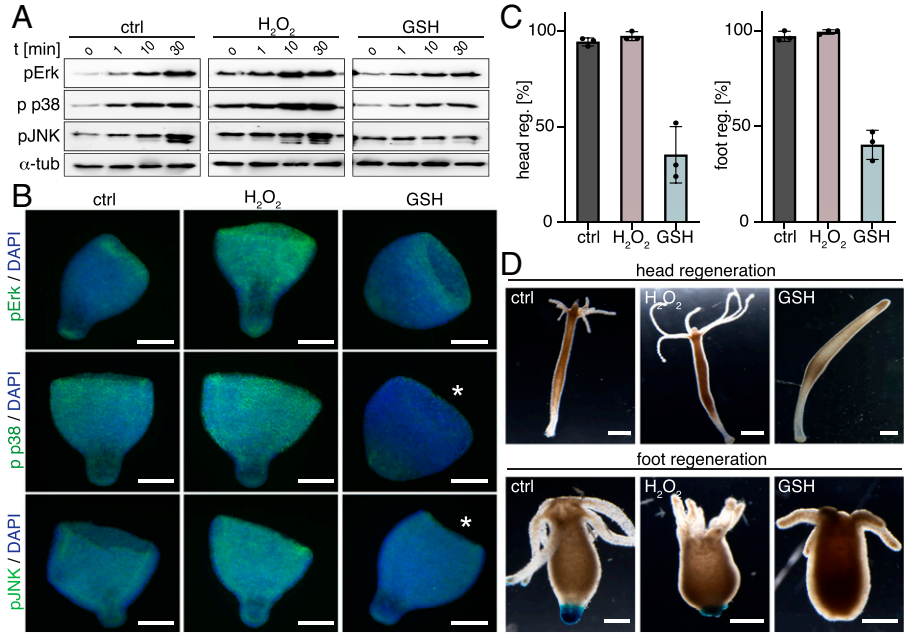

Fig. 2. MAPK activation acts downstream of redox signaling. (*A* and *B*) Analysis of ROS in regenerating tissue within the first 30 min postamputation. Polyps were bisected at 50% body length and allowed to regenerate in the presence of HM (ctrl) or HM supplied with either H_2O_2 or GSH. Asterisks indicate decreased staining intensity upon GSH treatment. Specimens were analyzed by western blot (*A*) or IF (*B*) using phospho-specific antibodies as indicated. (*A*) Exposure to H_2O_2 increased activated MAPKs levels as compared with untreated ctrl, while regenerates in reduced GSH showed less MAPK activation. (*B*) IF analysis of polyps fixed at 30 min postamputation showed an increase in MAPK activation after H_2O_2 treatment and a decrease after reduced GSH treatment. Scale bars: 250 μm. (*C*) Quantitative analysis of polyps bisected at 50% body length. 72 h after the onset of regeneration, ctrl polyps and H_2O_2-treated animals regenerated normally, whereas GSH exposure inhibited both head and foot regenerates. Error bars indicate the mean of three independent experiments with SD. $n = 45$ per condition. (*D*) Representative images of the experiment described in *C*. Regeneration of a head or foot was evaluated as before (Fig. 1*E*). Scale bars: 500 μm.

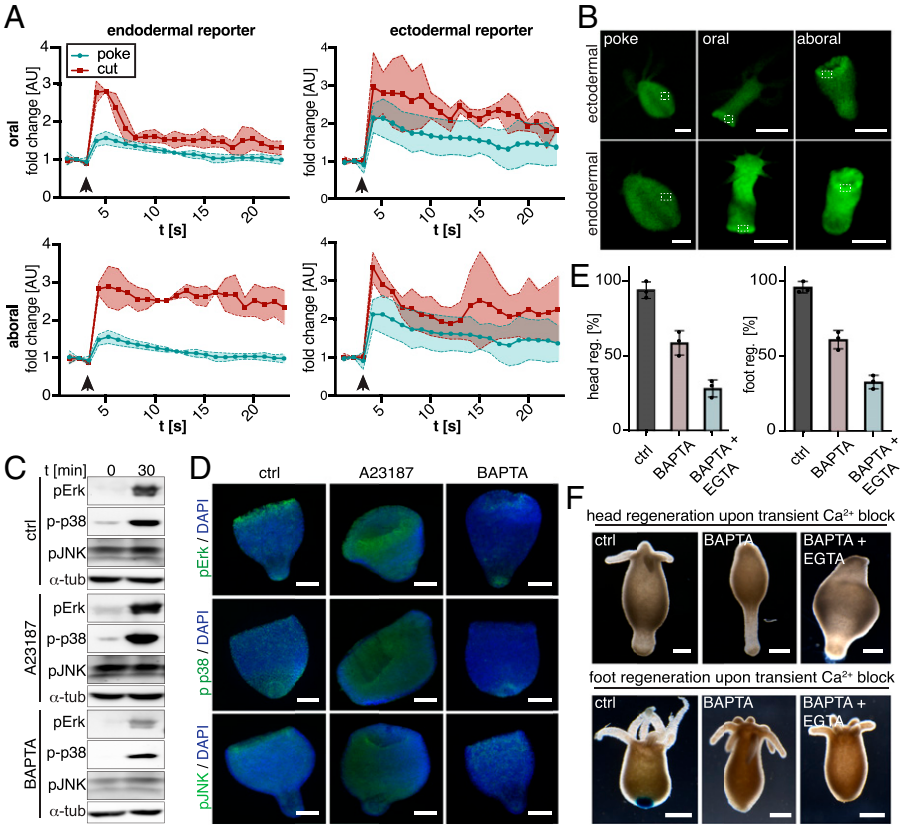

Fig. 3. MAPK activation is calcium dependent. (*A*) Injury causes increased and prolonged calcium release. Using transgenic ectodermal and endodermal GCaMP reporter strains, Ca^{2+} release was measured *in vivo* by fluorescence increase (arbitrary units [AU], i.e. fold change increase of basic reporter activity) after cutting (injury) or touch-induced contraction (noninjury). The time point of the poke or cut is indicated by an arrowhead. Mechanically stimulated ctrl polyps show a brief increase in fluorescence in both germ layers, whereas cut polyps show a prolonged increase in signal activity. Note that this increase occurs at both the oral and the aboral sites of section. (*B*) Representative pictures of transgenic Ca^{2+} reporter strains at 5 s postamputation. Dashed boxes indicate regions used for measurements shown in *A*. Scale bars: 500 μm. (*C* and *D*) Changes in intracellular Ca^{2+} levels affect MAPK activation, as analyzed by western blots (*C*) or by IF (*D*). (*C*) Animals were sectioned in the presence of the intracellular calcium chelator BAPTA, the ionophore A23187, or DMSO (ctrl). Whole-body lysates were prepared at 30 min pi and subjected to western blot analysis using phospho-specific MAPK antibodies. A decrease of Ca^{2+} (BAPTA) resulted in a decrease in activated MAPK levels, while an increase of Ca^{2+} (A23187) resulted in elevated phosphorylation events of all MAPKs. (*D*) IF analysis of whole-mount polyps after exposure to DMSO (ctrl), A23187, or BAPTA. Animals were fixed 30 min after amputation and stained with antibodies specific for pERK, pp38, and pJNK. Increasing cytoplasmic calcium levels transformed the gradient-like distribution of activated MAPKs (ctrl) into a homogenous staining throughout the tissue (A23187). Calcium capture by BAPTA resulted in a reduction of signal intensity upon injury. Scale bars: 250 μm. (*E* and *F*) Calcium release is essential for regeneration. Bisected polyps were exposed to DMSO, BAPTA, or BAPTA/EGTA for 3 h after cutting, and the regeneration capacity was evaluated at 72 hpa. The transient repression of Ca^{2+} signaling by BAPTA inhibited head and foot regeneration significantly ($n = 40$ each; error bars indicate the mean of three independent experiments with SD). Note that regeneration was further reduced when BAPTA was used in combination with EGTA. (*F*) Representative images of the experiment described in *E*. Scale bars: 500 μm.

patterning in *Hydra* (23). Upon decapitation, multiple Wnt ligands are transcriptionally activated in the head regenerate in a temporal sequence (27). However, only little attention has been paid to factors governing foot regeneration. Recent results showed that expression of β-catenin is crucial for both head and foot regeneration—a novelty, as β-catenin had been assumed to act solely on head regeneration (32). We therefore asked whether Wnt signaling is likewise activated in response to injury in a position-independent manner, as observed for MAPKs in this study and as reported for β-catenin elsewhere.

For this, tissue of head and foot regenerating tips was collected at different time points to examine the expression levels of *Wnt3*, *Wnt9/10c*, and *Wnt7* by qRT-PCR analysis (Fig. 4*A*). The selection was based on our previous in situ hybridisation and transcriptome studies, which revealed that *Hydra Wnt9/10c* and *Wnt3* were expressed within the first 3 h of head removal, making them the earliest *Wnt* genes, while *Wnt7* expression started much later, at 12 h (27, 37). In line with this, our qRT-PCR analysis showed an up-regulation of *Wnt9/10c* and *Wnt3* after 3 hpa, while the response of *Wnt7* was minimal during the first 6 hpa (Fig. 4*B*). This up-regulation was detectable in both head and foot regenerates, although it was less pronounced in the regenerating foot tissue. While *Wnt3* and *Wnt9/10c* expression was sustained in regenerating head tissue at 6 hpa, it started to significantly drop in foot regenerates, suggesting that positional specification occurs as early as 6 hpa (Fig. 4*B* and *SI Appendix*, Table S1*A*).

We next wanted to clarify whether these diverging kinetics of *Wnt* expression upon amputation were associated with specific functions in head patterning. To this end, small interfering RNA (siRNA) mediated knockdowns of *Wnt3*, *Wnt9/10c*, and *Wnt7* were performed in order to examine the role in head and foot regeneration upon bisection (Fig. 4 *C*–*E* and *SI Appendix*, Fig. S6 and Table S1*B*). The capacity to form a head or foot dropped to about 50% after knockdown of *Wnt3*-, *Wnt9/10c*-, and si*Wnt7*-treated animals in both head and foot regenerates. While foot regeneration was completely abrogated independent of the targeted *Wnt* gene, silencing of *Wnt9/10c* in head regeneration resembled the phenotype observed upon MAPK inhibition; i.e., animals showed normal wound healing but no signs of regeneration (Fig. 4*E*). By comparison, *siWnt3*-treated animals appeared initially to regenerate but then exhibited a peculiar phenotype without mouth and tentacles; instead, they formed a large monotentacle (Fig. 4*E*). Knockdown of *Wnt7* showed a less severe phenotype characterized by mispositioned tentacles along the hypostome. These data clearly indicate that early *Wnt* genes, particularly *Wnt9/10c* and *Wnt3*, are required for the onset of regeneration and head patterning, while later *Wnts*, such as *Wnt7*, are more involved in fine-tuned, small-scale patterning. The fact that the phenotype for *Wnt3* knockdown is not a complete absence of regeneration, as observed for *Wnt9/10c*, suggests that Wnt9/10c is required for the onset of regeneration immediately after wound healing, while Wnt3 is involved in the initial specification of head identity. In contrast, expression of *Wnt* genes in foot regenerates seems to be essential to initiate the onset of regeneration, while later patterning and specification are accomplished by further factors.

MAPKs Enable Wnt Signaling. Given our results that MAPK activation occurs in a position-independent manner in response

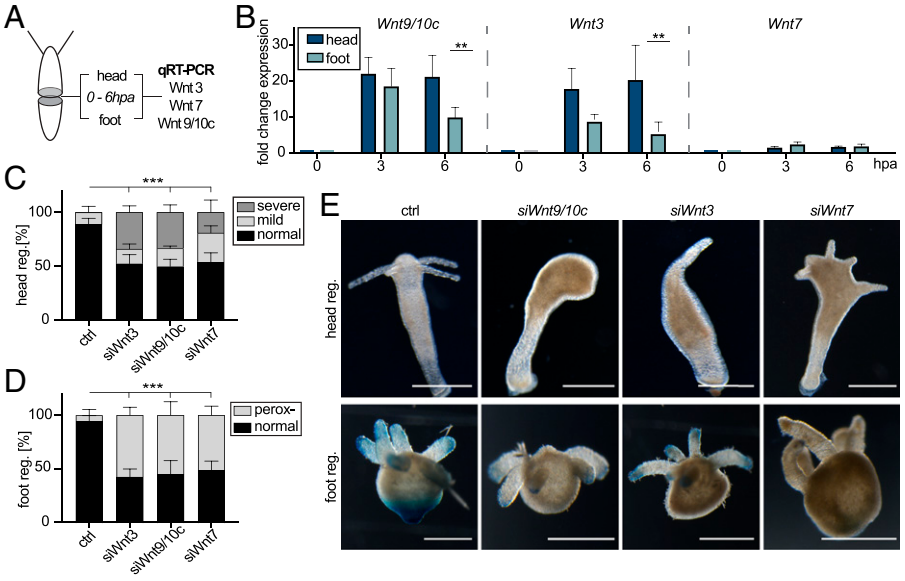

Fig. 4. Wound- and patterning-specific functions of Wnts. (*A*) Activation of *Wnt* expression in head and foot regenerates of bisected polyps. RNA was isolated from tissue of bisected polyps at the indicated time points and used for qPCR analysis with specific primers for *HyWnt9/10c*, *HyWnt3*, and *HyWnt7*. Values obtained were normalized to the *GAPDH* ctrl, and fold changes were calculated. (*B*) Expression levels of *HyWnt3* and *HyWnt9/10c* increased about 20-fold within the first 6 h in both head and foot regenerates upon injury, while the *HyWnt7* increase was only twofold. Note that the foot-specific decrease of *Wnt* expression is already initiated at 6 hpa. Significance was tested using Student's *t* test. $^{**}P < 0.005$. Error bars without asterisks did not pass the significance threshold. (*C–E*) siRNA-mediated knockdown of *Wnt3*, *Wnt9/10c*, and *Wnt7* results in decreased regeneration capacity. (*C*) Silenced polyps were bisected, and head regeneration was evaluated at 72 hpa. The regeneration capacity of polyps dropped to about 50%, with *siWnt3* and *siWnt9/10c* treatment affecting the onset of regeneration, while *siWnt7* caused patterning defects. (*D*) Regeneration capacity upon *Wnt3*, *Wnt9/10c*, or *Wnt7* knockdown equally decreased to less than 50% in foot regenerates determined by peroxidase assay (perox-). Error bars indicate the mean of five independent experiments with SD. Head regeneration: *n* (siGFP) = 163, *n* (*siWnt3*) = 153, *n* (*siWnt7*) = 140, *n* (*siWnt9/10c*) = 154. Foot regeneration: *n* (siGFP) = 95, *n* (*siWnt3*) = 92, *n* (*siWnt7*) = 92, *n* (*siWnt9/10c*) = 90. Significance of regeneration capacity was tested using logistic regression analysis, $^{***}P < 0.001$. (*E*) Representative pictures of *C* and *D* are shown. *siWnt9/10c* blocked regeneration completely, while *siWnt3*-treated head regenerates formed a characteristic monotentacle and *siWnt7* treatment resulted in misaligned tentacles. Foot regeneration was abrogated in all *Wnt*-silenced polyps, as determined by peroxidase assay. Scale bars: 500 μm.

to injury, we asked whether ERK, p38, or JNK affects early expression of *Wnt3* and *Wnt9/10c*. To this end, animals were bisected at 50% body length and evaluated by qRT-PCR in controls and upon MAPK inhibition at different time points postamputation. We decided to investigate the expression levels of *Wnt3* and *Wnt9/10c* genes only, since they were most implicated in the onset of regeneration (Fig. 4). Upon inhibition of the p38 or JNK pathways (i.e., the stress-induced MAPK pathways), *Wnt3* was strongly up-regulated in a position-independent manner in head and foot regenerates (Fig. 5 *A* and *B*, *Left* and *SI Appendix*, Table S1 *C* and *D*). This up-regulation of *Wnt3* was, however, accompanied by strong down-regulation of *Wnt9/10c* in head and foot regenerates (Fig. 5 *A* and *B*, *Right*). Thus, p38 and JNK have opposing effects on early *Wnt9/10c* and *Wnt3* gene regulation. By comparison, ERK inhibition had only a mild repressive effect on *Wnt3* in head regenerates, while foot regenerates were unaffected. Also, there was a discernible difference in the repression of *Wnt9/10c* in foot and head regenerates, suggesting a different responsiveness of the tissues for ERK-induced Wnt activation (Fig. 5 *A* and *B* and *SI Appendix*, Table S1). Because animals that were inhibited for p38 or JNK do not show any signs of regeneration despite the increased expression levels of *Wnt3*, we conclude that *Wnt9/10c* acts as the primary *Wnt* gene in the transcriptional cascade during regeneration. This is also confirmed by the more pronounced phenotype of the *Wnt9/10c* knockdown as compared to the other Wnts (Fig. 4 *C–E*).

To test whether the regeneration deficiency upon MAPK inhibition, as shown in Fig. 1*F*, is a direct consequence of aberrant Wnt signaling, we repeated the regeneration assay in the presence of MAPK inhibitors and examined whether recombinant *Hydra* Wnt3 or Wnt9/10c protein is able to restore the regeneration capacity (Fig. 5*C* and *SI Appendix*, Fig. S7). Our previous work has shown that treatment of a regeneration-deficient strain with recombinant Wnt3 can rescue regeneration, likely by the activation autocatalytic Wnt activation loop in regenerates (26, 27). In Dimethyl sulfoxide (DMSO) treated control polyps, neither Wnt3 nor Wnt9/10c treatment showed any effect on the progression of regeneration. In ERK- and p38-inhibited polyps, we found an increase of regenerating animals after Wnt treatment, with Wnt9/10c consistently having a stronger effect than Wnt3 (*SI Appendix*, Fig. S7). This is line with our previous finding that *Wnt9/10c* is more strongly repressed by p38/ERK inhibition than *Wnt3*. Neither Wnt3 nor Wnt9/10c was able to restore regeneration upon JNK inhibition (Fig. 5*C* and *SI Appendix*, Fig. S7 and Table S1*E*). This might be due to JNK's pleiotropic functions in noncanonical Wnt signaling, e.g., during tentacle morphogenesis (17).

The fact that Wnt3 and Wnt9/10c are both required to initiate regeneration raised the question of whether Wnt3 and Wnt9/10c solely act on the onset of regeneration or also fulfill instructive functions in the patterning process, as initially postulated for Wnt3 (23). We tested this assumption by treating gastric pieces with the recombinant *Hydra* Wnts. To do so, we cut out the middle gastric pieces without head and peduncle and incubated them with recombinant *Hydra* Wnt3, Wnt9/10c, a 1:1 combination of both, or Bovine serum albumin (BSA) as a control (Fig. 5*D*). While BSA-treated pieces regenerated normally, 35% of the regenerates that were treated with recombinant Wnt formed heads at both ends of the body column (Fig. 5 *E* and *F* and *SI Appendix*, Table S1*F*). Of those regenerates, 32% showed ectopic tentacles or double heads. The fact that at the aboral end a head instead of the presumptive foot was formed suggests a change in the axial identity of the regenerating tissue similar to a polarity reversal induced by parabiosis with head tissue in transplantation experiments (54). This effect was stronger with Wnt3 than with Wnt9/10c and strongest with the combination of both (Fig. 5*E*). The foot was formed centrally and thus most distally in relation to the heads, an effect that likely corresponds to proportion regulation (55–57).

When we blocked β-catenin signaling by (5Z)-5-{[2,5-Dimethyl-1-(3-pyridinyl)-1H-pyrrol-3-yl]methylene}-3-phenyl-1,3-thiazolidine-2,4-dione (iCRT14) treatment at various stages after amputation in order to elucidate early and late Wnt/β-catenin effects of head and foot regenerates, we found strong dependence of late head regeneration on Wnt-dependent transcription and

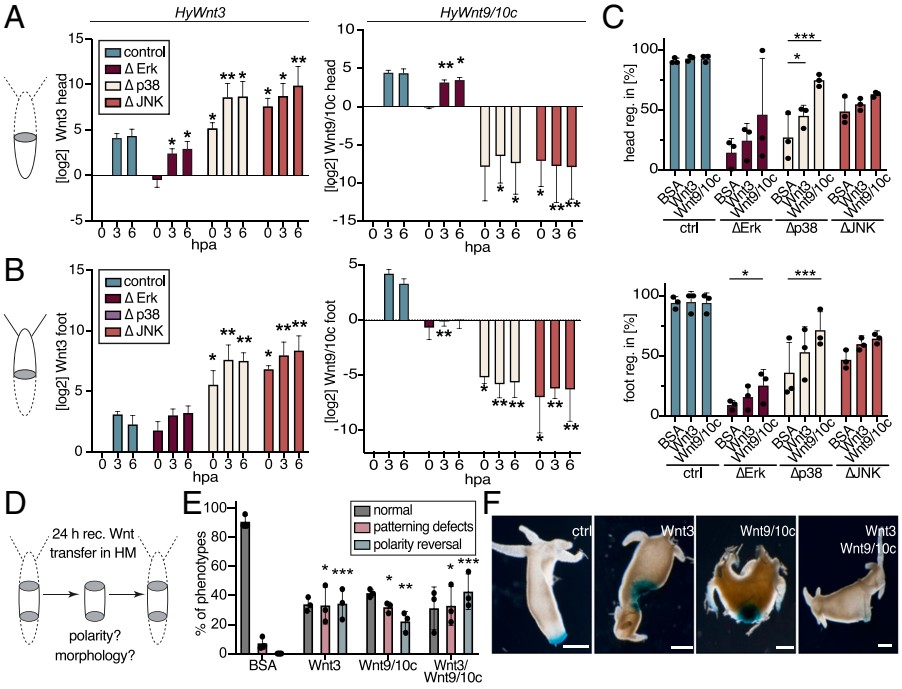

Fig. 5. MAPKs influence *Wnt* expression levels in head and foot regenerates. (*A*) Activation of *Wnt* expression in head and foot regenerates of bisected polyps. RNA was isolated from tissue of bisected polyps at the indicated time points and used for qPCR analysis with specific primers for *HyWnt3* and *HyWnt9/10c*. Head (*A*) and foot (*B*) regenerating polyps were incubated with inhibitors specific to each MAPK, and log2 fold change was calculated. While inhibition of ERK activity resulted in reduced *Wnt* expression, inhibition of stress-induced MAPKs yielded higher expression levels for *Wnt3* but down-regulation for *Wnt9/10c*. Error bars indicate the mean of three independent experiments with SD. Significance was tested using Student's *t* test. $*P < 0.05$; $**P < 0.005$. Error bars without asterisks did not pass the significance threshold. (*C*) HyWnt9/10c partially rescues regeneration defects after MAPK inhibition. Polyps were bisected and regenerated in the presence of inhibitors specific to either ERK, p38, or JNK. During the first 24 h, regenerates were incubated with recombinant HyWnt3, HyWnt9/10c, or BSA (ctrl). At 72 hpa, an increased regeneration capacity was found after HyWnt9/10c treatment for ERK- and p38-inhibited polyps, whereas the effect of HyWnt3 treatment was smaller. Error bars indicate the mean of three independent experiments with SD. Significance of regeneration restoration was tested using logistic regression analysis. $*P < 0.05$; $**P < 0.005$; $***P < 0.001$. Absolute numbers and representative pictures of animals used are shown in *SI Appendix*, Fig. S7. (*D*) Schematic representation of the polarity reversal experiment performed in *E* and *F*. A central piece of gastral tissue was excised from budless animals at 30**%** and 70**%** body length, exposed to recombinant Wnt protein for 24 h, and afterward allowed to regenerate in HM for 6 days. (*E*) Polyps were scored at 7 days postamputation. Pieces incubated with BSA regenerated animals with the original oral-aboral polarity. Pieces incubated with HyWnt3 and/or HyWnt9/10c regenerated animals with morphological defects (e.g., ectopic tentacles) and animals in which a head formed at the original oral and aboral pole, indicating a transformation of positional identity (polarity reversal) at the aboral end. Pieces with polarity reversal form foot structures between the two heads, as visualized by peroxidase assay. Note that polarity reversal is less pronounced in polyps exposed to HyWnt9/10c only. Error bars indicate the mean of three independent experiments with SD. Significance was determined by binomial regression model. $*P < 0.05$; $**P < 0.005$; $***P < 0.001$. *n* (BSA) = 61, *n* (Wnt3) = 72, *n* (Wnt9/10c) = 78, *n* (Wnt3/Wnt9/10c) = 79. (*F*) Representative pictures of the experiment described in *E*. Regenerates incubated with BSA (ctrl) show a correct oral-aboral axis, while regenerates treated with Wnt proteins show polarity reversal. Scale bars: 500 μm.

dependence of early head and early foot regeneration (*SI Appendix*, Fig. S6 *B* and *C*). In line with these data, it was also shown that Wnt3, Wnt9/10c, and Wnt7 decrease in expression in foot regenerates by 8 to 12 hpa (31). Thus, late patterning of regenerating feet must be accomplished by factors other than Wnts. These data clearly suggest that Wnt3 and Wnt9/10c possess stage-specific dual functions that comprise the position-independent onset of regeneration and the instructive function for head patterning. The latter was also evident from previous work linking Wnt signaling and oral pattern formation in *Hydra* (26–28).

Antagonistic Function of ERK and Stress-Induced MAPKs in Apoptosis. Our finding that ERK and the stress-induced MAPK pathways exhibit complementary effects on *Wnt* expression suggests that these pathways are integrated by positive and negative feedback mechanisms during *Hydra* regeneration. We therefore tested such putative feedback interactions by using pathway-specific inhibitors. For this purpose, animals were incubated with one of the inhibitors for 1 h and bisected. At different time points after sectioning, the regenerates were then tested for the levels of activated MAPKs by IF and western blot analyses. Our data indicate positive feedback between the stress-activated p38 and JNK pathways and antagonism between stress-activated MAPKs and the ERK pathway, as summarized in Fig. 6*A*. IF analysis reveals that ERK phosphorylation was inhibited by pretreatment with the MEK/ERK inhibitor; however, pERK was activated in response to treatment with the p38 inhibitor or, to a lesser extent, the JNK inhibitor (*SI Appendix*, Fig. S8*A*). The stress-activated MAPKs, i.e., p38 and JNK, showed increased activation levels upon ERK inhibition, whereas a reduction was obtained for pJNK in the presence of the p38 inhibitor and likewise for pp38 upon exposure to the JNK inhibitor. IF-based inhibitor analysis was fully confirmed by the corresponding western blot data (*SI Appendix*, Fig. S8*B*).

Strikingly, the mutual antagonism between the p38 and ERK pathways exhibited the strongest regeneration phenotypes upon inhibition (Fig. 1 *F* and *G*). Although MAPKs control many cellular processes, one major antagonistic function is their role in cell survival and apoptosis (58). We therefore next analyzed whether there is a link between MAPK activation and the induction of apoptosis. We studied apoptosis by using a standard Terminal deoxynucleotidyl transferase dUTP nick end labeling (TUNEL) staining protocol, thereby avoiding a heating step to increase signal intensity, which in our hands led to staining artifacts (*Materials and Methods* and Fig. 6*B*). Apoptotic cells were located close to the amputation site, whereas the remaining tissue was virtually free of apoptotic cells (Fig. 6*C*). In bisected animals, apoptotic cells were found in tissue regenerating a head and foot, i.e., at both sites of cutting. This finding is consistent with recent work of the Juliano laboratory (31), which used acridine orange staining to detect apoptotic events in regenerates. We detected apoptosis as early as 60 min after amputation, reaching its maximum at 1 to 2 hpa and dropping again by 3 hpa (Fig. 6*C*). The number of TUNEL-positive cells increased strongly upon inhibition of the JNK pathway but was completely diminished after ERK inhibition, while no significant change was detectable after inhibition of p38. This indicates an early antiapoptotic function of JNK and a proapoptotic function of ERK (Fig. 6*D*).

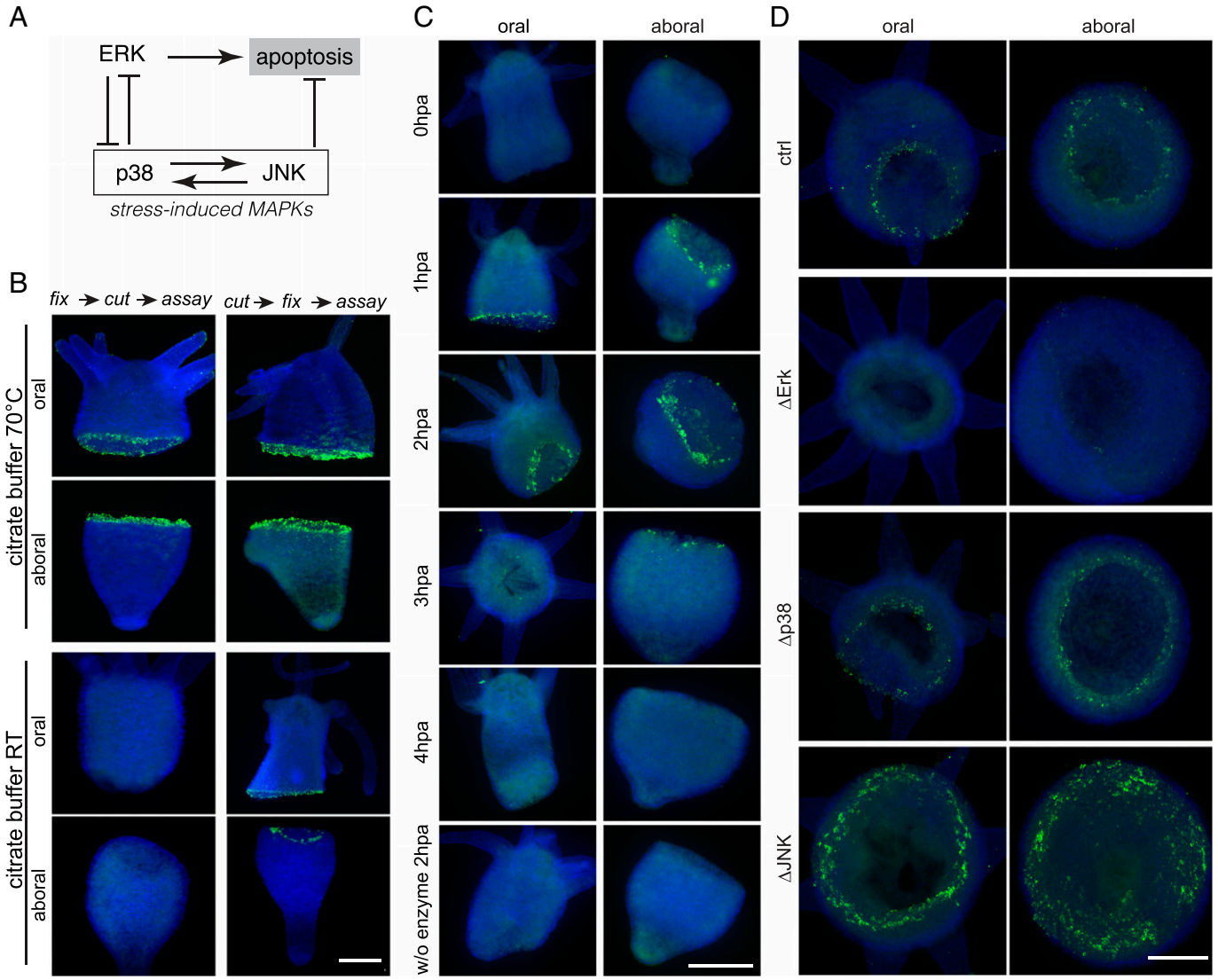

Fig. 6. MAPK cross talk balances apoptosis. (*A*) Scheme showing the relationships between MAPK pathways based on data shown below and in *SI Appendix*, Fig. S8. While stress-activated MAPKs (p38 and JNK) activate the respective pathway, the ERK pathway inhibits stress-activated MAPKs. Antagonism between ERK and JNK pathways is reflected on the level of apoptosis. (*B*) Comparison of protocols provided by the manufacturer and as published in Vogg et al. (25) and Chera et al. (29). Specificity of the TUNEL reaction was tested by comparing polyps that had been fixed overnight, followed by amputation to animals that had been first bisected and subsequently fixed. *Upper*: Incubation step at 70 °C yielded the same rate of TUNEL-positive cells in animals fixed before and after amputation. Therefore, the signal was considered to be unspecific, and incubation of polyps in citrate buffer was executed exclusively at room temperature to prevent an unspecific stain despite the decreased signal intensity (*Lower*). Scale bars: 250 μm. (*C*) Time lapse of apoptosis visualized by TUNEL assay from bisected polyps fixed at the indicated time points. The maximum of apoptotic cells is detectable between 1 and 2 hpa in both head and foot regenerates. Scale bars: 250 μm. (*D*) Visualization of apoptotic cells by TUNEL assay analysis in bisected polyps upon inhibition of MAPKs at 1.5 hpa. While p38 inhibition has no effect on apoptotic events, the frequency clearly increased upon JNK inhibition and was diminished in the presence of the ERK inhibitor. Note that there is no difference between head and foot regenerates. Scale bars: 250 μm. Nuclei were stained with DAPI (blue) in all shown images.

The antagonistic role of the stress-inducible MAPKs and ERK in apoptosis is part of a general injury response during *Hydra* regeneration. This is reminiscent of signal integration by MAPKs in development and cancer formation of vertebrates (58–60). We assume that the antagonism between ERK and JNK/p38 pathways in apoptosis and Wnt signaling has a balancing function in regulating cell fitness and survival to ensure tissue health at the onset of regeneration (Fig. 6*A*).

Discussion

Wnt signaling is an animal-specific pathway with multiple functions in cell proliferation, stem cell maintenance, tissue polarity, and development (61–63). Wnts have been associated with wound healing already in early studies, where an up-regulation of *Wnt4* upon injury was discovered in the murine epidermis (64). This assumption was confirmed by further discoveries in different model systems reporting an initial up-regulation of *Wnt* expression in response to injury, as in *Hydra* (23), planarians (65), and vertebrates (66–68). Yet the mechanism by which *Wnt* expression is initiated upon injury remained largely elusive. In this study, we demonstrate that Wnt is activated in an early injury response downstream of MAPKs that are initiated by ROS and calcium release within minutes after wounding. Our findings are in line with previous findings demonstrating that injury releases signals indispensable for regeneration in intact (33, 34) and regeneration-deficient *Hydra* (35). The importance of the injury signal is likely due the default activation of Wnt/β-catenin signaling, as presented in this study and in Gufler et al. (32).

Signaling Architecture of the Hydra's Generic Wound Response. Our data show that injuries quickly lead to phosphorylation of MAPKs in ectodermal and endodermal epithelial cells. We were able to demonstrate that the injury signal is composed of Ca^{2+} and the production of ROS, which has not been studied in early *Hydra* regenerates so far (32). Both signals transmit information about tissue damage intracellularly by activating ERK, JNK, and p38. The activation by ROS is likely achieved by inactivation of counteracting protein tyrosine phosphatases via oxidation of regulatory cysteines, while calcium has been frequently reported to activate MAPK via calmodulin-dependent kinases, Protein kinase C (PKC), and Ras activation (69–72). Although there is increasing evidence for the importance of either ROS or calcium signaling upon injury, it is unclear whether ROS production is Ca^{2+} mediated or whether both messengers act independently in the regenerative context, as was shown for zebrafish fin regeneration (53).

MAPK phosphorylation was among the earliest regeneration responses in our previously shown proteomic/transcriptomic profile of *Hydra* head regeneration (37). In the present study, we show that the activation of ERK, p38, and JNK is essential for both head and foot regeneration, with ERK showing the most sustained activation kinetics (*SI Appendix*, Fig. S2). Since MAPK phosphorylation was observed upon both incision and amputation, irrespective of localization, it implicates MAPKs as part of a generic wound response. This term was initially brought up by Reddien and colleagues (11, 73), who showed that both forms of injury promote a position-independent up-regulation of the same set of genes in planarians. The finding was further specified by studies showing a sustained increase in pERK in response to incision and amputation, which was required for Wnt activation (74). In contrast, the role of stress-induced MAPK pathways in regeneration is only poorly investigated. Joint activation of both stress-inducible MAPK pathways was so far only reported for axonal regeneration in *Caenorhabditis* and imaginal disk regeneration in *Drosophila* (75, 76). While most studies focus on either ERK activation during regeneration (74, 77–79) or p38/JNK (9, 80), our data indicate that these pathways do not work independently of one another but are based on extensive cross talk. Inhibitor experiments revealed that p38/JNK interacts with ERK as a potential antagonist.

This antagonism of p38/JNK and ERK was also reflected on the level of apoptosis induction. Surprisingly, JNK exhibited anti-apoptotic and ERK exhibited proapoptotic properties (Fig. 6). While the two-sided face of JNK in apoptosis has been extensively described in various systems, the proapoptotic role of ERK has only started to raise awareness. It has been suggested that the anti-apoptotic role of JNK is based on the phosphorylation of the proapoptotic Bcl-2, which leads to its sequestration and thus inactivation (81). Interestingly, this family has been recently identified in *Hydra* and demonstrated to execute similar functions (82).

Conversely, although ERK has been frequently associated with antiapoptotic functions, a constantly growing number of studies have demonstrated ERK promotes proapoptotic processes as well (59). This phenomenon was observed in particular after ROS release, which leads to sustained ERK activation (83), as was also observed in this study. A sharp decrease in the number of apoptotic cells was also described by Chera et al. (40) for *Hydra* head regeneration. However, our data differ in that ERK-mediated apoptosis is not restricted to head regenerates but also occurs in foot regenerates (Fig. 6). The fact that ERK-mediated apoptosis occurs in response to injury, regardless of the amputated axial position, also challenges the earlier report by Chera et al. (29), in which apoptotic cells were described to occur exclusively at the oral-facing wound sites. We show that applying a standard protocol that omits a high-temperature incubation step, as used by Chera et al. (29), is not prone to yield unspecific signals, as shown for fixed samples (Fig. 4*B*). Our findings are also in full accordance with recent results by Cazet et al. (31), showing that the response to amputation is identical at both wounds and includes widespread apoptosis. Thus ERK-mediated apoptosis must be considered as an essential part of the generic wound response in Hydra.

Wnt9/10c and Wnt3 Are MAPK-Linked Members of the Generic Wound Response. Our previous data have revealed not only unexpected complexity between the early proteomic responses and the first transcriptional activation of the patterning GRNs (37) but also dominance of Wnt signaling in the formation of the early *Hydra* head organizer (21, 23, 24, 27, 37). It was therefore striking that two of the earliest and one of the latest *Wnt* genes (27) were activated in both head and foot regenerates. This is consistent with recent findings in *Hydra* (31, 32) indicating position-independent activation of Wnt signaling during regeneration, and it challenges the concept of an initial asymmetry of canonical Wnt signaling (29). As in planarians (11), it also raises the general questions of how the positional information is established and what function early *Wnt* genes have.

The fact that MAPKs are essential for *Hydra* regeneration (Fig. 1) and the discovery in planarians that *Wnt1* expression decreases with attenuated ERK activity (74) led us to systematically investigate the relationship between MAPKs and Wnts. When we tested the influence of ERK, p38, or JNK activation on the expression of the early regeneration genes *Wnt3* and *Wnt910c*, we found strong evidence that early *Wnt* expression is highly dependent on MAPK activation and largely independent of the axial position, i.e., the regeneration of a head or foot (Fig. 5 *A* and *B*). Consequently, MAPKs and early Wnts are part of a generic wound response that only becomes head organizer specific at about 6 hpa (Fig. 5). This is also supported by recent RNA sequencing (RNA-seq) data demonstrating that early gene expression is indistinguishable in presumptive head and foot tissue and only becomes position specific at 8 hpa (31). It also coincides with less pronounced effects of MAPK inhibition on *Wnt* expression at later stages (*SI Appendix*, Table S1 and Fig. 5 *A* and *B*).

Because prominent downstream effectors of MAPK signaling are transcription factors (TFs), we performed an in silico promotor analysis of *Wnt3, Wnt9/10c,* and *Wnt7* for TF binding sites associated with MAPK signaling (*SI Appendix*, Fig. S9*A*). All *Wnt* promotors showed high probability scores for the bZIP family of TFs such as cFos and different other CREB/ATF members (*SI Appendix*, Fig. S9*A* and Table S2). While cFos is a downstream target of the ERK pathway, ATFs can be activated by the JNK or p38 pathway (84–86). This hypothesis is further supported by recent assays for transposase accesible chromatin sequencing (ATAC-seq) studies in *Hydra* demonstrating that early stages of injury-induced *Wnt* expression likely depend on bZIP TFs such as cFos and ATFs (31). In silico analysis revealed that ATF2/CREB can bind mainly to the *Wnt9/10c* promotor and ATF3 can bind mainly to the *Wnt3* and *Wnt7* promoters (*SI Appendix*, Table S2). ATF3 is activated in response to stress stimuli (87–90) but has not been described in cnidarians (*SI Appendix*, Fig. S10) (91). In electromobility shift assays (EMSAs), we found that recombinant human ATF3 binds to the putative ATF3 binding sites of the *HyWnt3* promoter (*SI Appendix*, Fig. S9*B*). Although we

cannot rule out the possibility that ATF2/CREB also binds to the putative ATF3 sites, differential binding of ATF2/CREB and ATF3 to the promoter region of *Wnt9/10c* and *Wnt3* could explain the antagonistic effects of MAPKs on *Wnt* expression. We therefore propose a model in which differential binding of ATFs promotes the expression of *Wnt9/10c* to initiate regeneration and prevent premature up-regulation of patterning Wnts such as *Wnt3* and *Wnt7*. To our knowledge, there are currently only two reports of ATF2-driven expression of *Wnts,* i.e., in colon cancer cells (92) and in hematopoietic tumor cells (93), and none on ATF3. For us, they represent a level of *Wnt* regulation that has received little attention but is important for integrating Wnts in the generic wound response.

β-Catenin and Wnt Levels Determine the Patterning Fate in Regenerates. While the differential activation of Wnts by ATFs is still part of the injury-induced cascade, the question remains how the transition from a generic wound response to position-specific gene expression is achieved on the cellular level. Previous work in *Hydra* (23, 94, 95) and *Nematostella* (22, 96), as well as related studies in planarians (65, 97, 98), has convincingly shown that β-catenin is crucial for the overall polarity of the body (99). We thus assume that β-catenin is intimately linked to the long-term storage of the body axis gradient, as already postulated (100, 101). This gradient is known as head-forming competence and shown to be different at various axial levels along the oral-aboral body axis in *Hydra* (95). It was introduced as the source density in the mathematical model by Gierer and Meinhardt (102) and is proposed to be essential for establishing the previous positional identity. Since the source density seems to encode a distinct responsiveness/competence along the body axis, we hypothesize that the specification of head and foot tissue occurs by the interplay of the injury signal with the source density.

We tested the role of injury-induced self-amplification of Wnt/β-catenin signaling in the context of bud formation. Since this process requires high levels of β-catenin (94), we placed an incision in the budding region at a fluorescently labeled side to examine whether we are able to artificially induce budding (Fig. 7*A*). Compared to a noncut control, the frequency of bud development at the site of incision increased from 20 to 60% (Fig. 7*A* and *SI Appendix*, Table S1*G*). This is in line with recent findings by Cazet et al. (31), who were able to induce ectopic head organizers by puncture wounds.

We also attempted to override a presumed existing positional gradient of the source density by incubating gastric pieces with the GSK3 inhibitor azakenpaullone, which generates high levels of β-catenin throughout the whole tissue (28, 33, 103). Strikingly, these regenerates formed heads at both ends of the body column to about 85% (Fig. 7*B*), which is twice as high compared to gastric tissue treated with recombinant Wnts (Fig. 5 *E* and *F*). This is strikingly similar to alsterpaullone- or azakenpaullone-treated embryos of the sea anemone *Nematostella*, which also form polyps with a head at both ends of the body axis (22), an approach that has also recently been used to identify β-catenin downstream targets patterning the oral-aboral axis in these animals (96).

These experiments demonstrate that *Wnt/β-catenin* signaling is intimately linked to the level of the source density, which in turn determines the fate of the regenerating *Hydra* tissue as initially shown for planarian regeneration (Fig. 7*C*). Recently proposed mathematical models support the importance of an initial injury signal and β-catenin for robust patterning in *Hydra* and animal regeneration (104–106). Given that injury-induced *Wnt* expression has already been described for the regeneration of fish fins, amphibian limbs, and mammalian intestine and heart, this activation loop seems to be a common strategy across metazoan phyla to overcome tissue damage in both regeneration-competent and regeneration-noncompetent organisms (107). We thus conclude that the injury response is essential to promote both wound healing and regeneration,

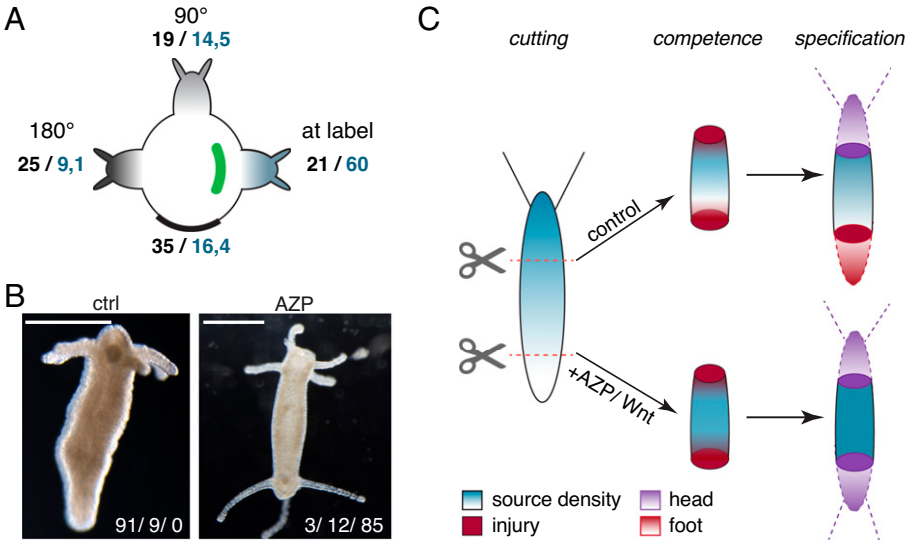

Fig. 7. Injury triggers default *Wnt* expression to initiate patterning. (*A*) Polyps were labeled with green fluorescent latex beads and subsequently incised in the budding region at the side of the label at 2 h postlabeling (cut), while the uncut population remained unaffected (ctrl). After 3 days, the number (ctrl/cut) and position of new buds were determined, as depicted by schematic representation. While noncut polyps exhibited random bud development, incised animals showed positional bias of budding at the labeled side. Significance of biased budding from three independent experiments was tested using logistic regression analysis with a *P* value of 0.0001. *n* (ctrl) = 48, *n* (cut) = 55. (*B*) Gastric pieces were excised and exposed to DMSO (ctrl) or to azakenpaullone (AZP). Stabilization of β-catenin yields 85% of animals showing head structures at both extremities upon AZP treatment, while ctrl polyps preserve the original polarity. *Right Lower Corner*: Numbers indicate the frequency of normal morphology/morphology defects/polarity reversal. Scale bars: 500 μm. *n* (ctrl) = 96, *n* (AZP) = 95. (*C*) Schematic representation of how source density is related to Wnt/β-catenin signaling and how it finally yields head and foot regeneration upon injury. Injury causes initial up-regulation of Wnt/β-catenin at either end that induces the tissue to regenerate. The positional specification of the regenerating tissue is dependent on the relative value of the source density along the body column. While high source density commits the tissue to head regeneration, lower values of the source density yield foot regeneration.

while the decision to regenerate or simply heal the tissue is determined by its competence. The nature of the source density, which encodes this competence, is still elusive, but our data stress the importance of identifying the molecular cues that constitute the source density and determine whether wound healing or regenerative pathways are activated upon injury.

Materials and Methods

***Hydra* Culture.** Polyps were kept in HM (1 mM $NaHCO_3$, 0.1 mM KCl, 0.1 mM $MgCl_2$, 1 mM $CaCl_2$, and 1 mM Tris, pH 6.9) at 18 °C. Animals were fed three times a week with *Artemia salina* nauplii. The medium was exchanged daily. The strain *Hydra vulgaris* AEP was used for all experiments if not otherwise indicated. Animals were starved for 24 h prior to experiments.

Inhibitor Treatments. Animals were pretreated with inhibitors for 1 h prior to the start of the respective experiment. 25 μM U0126 (MEK/ERK inhibition), 50 μM SB 203580 (p38 inhibition) (*SI Appendix*, Fig. S11), and 1 μM SP600125 (JNK inhibition) (21) were diluted in HM. All reagents were purchased from Cell Signaling Technology. All inhibitors were dissolved in DMSO as 20 mM stock solutions. For calcium experiments, 2 μM A23187 (Sigma-Aldrich) in HM was used if not otherwise indicated. 50 μM BAPTA and 0.5 mM EGTA were used in calcium-free HM. Both reagents were purchased from Sigma-Aldrich. BAPTA and A23187 were dissolved in DMSO as 50 mM stock solutions. For redox experiments, 100 μM freshly purchased GSH (Merck Millipore) and 500 μM H_2O_2 (Sigma-Aldrich) were diluted in HM. As shown before for U0126 (42), the effects of inhibitors are dose dependent and require activity control for long-term treatment of head and foot regenerates. Inhibitors and GSH were exchanged every 12 h. For reagents dissolved in DMSO, the solvent only served as control by diluting an equal volume of DMSO in HM. For multiple inhibitor experiments, the highest volume of the inhibitor solution was used as reference for the control.

Full details of methods are given in *SI Appendix, SI Material and Methods*.

Data, Materials, and Software Availability. All study data are included in the article and/or supporting information.

ACKNOWLEDGMENTS. S65 and S66 strains with the Act hyGCaMP reporter were established in cooperation with Jan-Marek Weislogel and Yukio Nakamura and provided by Hilmar Bading. We further acknowledge Ingrid Lohmann and Pedro Pinto for sharing their experience in EMSA, Maike Fath for her technical assistance, and Sigrid Grieser-Ade and Simone Wolters for their care of *Hydra* cultures. We thank Jack Cazet and Celina Juliano for critical comments on the first version of the manuscript and Hendrik Petersen and Bruno Gideon Bergheim for discussions. This work was supported by grants to A.M.-C. (German Research Foundation, SFB 1324-B05), S.O. (German Research Foundation, SFB 1324-B07), and T.W.H. (German Research Foundation, SFB 872-A1-2/3, German Research Foundation, SFB 1324-A5-1/2). An early version of the manuscript was deposited at the bioRxiv server (108).

1. K. D. Poss, Advances in understanding tissue regenerative capacity and mechanisms in animals. *Nat. Rev. Genet.* **11**, 710–722 (2010).
2. J. A. Goldman, K. D. Poss, Gene regulatory programmes of tissue regeneration. *Nat. Rev. Genet.* **21**, 511–525 (2020).
3. J. P. Brockes, A. Kumar, Appendage regeneration in adult vertebrates and implications for regenerative medicine. *Science* **310**, 1919–1923 (2005).
4. E. Bassat, E. M. Tanaka, The cellular and signaling dynamics of salamander limb regeneration. *Curr. Opin. Cell Biol.* **73**, 117–123 (2021).
5. E. M. Tanaka, P. W. Reddien, The cellular basis for animal regeneration. *Dev. Cell* **21**, 172–185 (2011).
6. A. Y. Wong, J. L. Whited, Parallels between wound healing, epimorphic regeneration and solid tumors. *Development* **147**, dev181636 (2020).
7. S. Vriz, S. Reiter, B. Galliot, Cell death: A program to regenerate. *Curr. Top. Dev. Biol.* **108**, 121–151 (2014).
8. C. P. Petersen, P. W. Reddien, Polarized notum activation at wounds inhibits Wnt function to promote planarian head regeneration. *Science* **332**, 852–855 (2011).
9. B. Tejada-Romero, J. M. Carter, Y. Mihaylova, B. Neumann, A. A. Aboobaker, JNK signalling is necessary for a Wnt- and stem cell-dependent regeneration programme. *Development* **142**, 2413–2424 (2015).
10. E. M. Hill, C. P. Petersen, Wnt/Notum spatial feedback inhibition controls neoblast differentiation to regulate reversible growth of the planarian brain. *Development* **142**, 4217–4229 (2015).
11. O. Wurtzel *et al.*, A generic and cell-type-specific wound response precedes regeneration in planarians. *Dev. Cell* **35**, 632–645 (2015).
12. A. G. Tewari, S. R. Stern, I. M. Oderberg, P. W. Reddien, Cellular and molecular responses unique to major injury are dispensable for planarian regeneration. *Cell Rep.* **25**, 2577–2590.e3 (2018).
13. M. Kragl *et al.*, Cells keep a memory of their tissue origin during axolotl limb regeneration. *Nature* **460**, 60–65 (2009).
14. J. H. Patel, P. A. Schattinger, E. E. Takayoshi, A. E. Wills, Hif1α and Wnt are required for posterior gene expression during Xenopus tropicalis tail regeneration. *Dev. Biol.* **483**, 157–168 (2022).
15. R. E. Harris, L. Setiawan, J. Saul, I. K. Hariharan, Localized epigenetic silencing of a damage-activated WNT enhancer limits regeneration in mature *Drosophila* imaginal discs. *eLife* **5**, e11588 (2016).
16. R. E. Harris, M. J. Stinchfield, S. L. Nystrom, D. J. McKay, I. K. Hariharan, Damage-responsive, maturity-silenced enhancers regulate multiple genes that direct regeneration in *Drosophila*. *eLife* **9**, e58305 (2020).
17. A. N. Ramirez, K. Loubet-Senear, M. Srivastava, A regulatory program for initiation of Wnt signaling during posterior regeneration. *Cell Rep.* **32**, 108098 (2020).
18. A. Trembley, *Mémoires pour servir à l'histoire d'un genre de polypes d'eau douce à bras en forme de cornes* (J.& H. Verbeek, Leide, 1744).
19. H. R. Bode, Head regeneration in Hydra. *Dev. Dyn.* **226**, 225–236 (2003).
20. T. W. Holstein, E. Hobmayer, U. Technau, Cnidarians: An evolutionarily conserved model system for regeneration? *Dev. Dyn.* **226**, 257–267 (2003).
21. I. Philipp *et al.*, Wnt/beta-catenin and noncanonical Wnt signaling interact in tissue evagination in the simple eumetazoan Hydra. *Proc. Natl. Acad. Sci. U.S.A.* **106**, 4290–4295 (2009).
22. C. Guder *et al.*, The Wnt code: Cnidarians signal the way. *Oncogene* **25**, 7450–7460 (2006).
23. B. Hobmayer *et al.*, WNT signalling molecules act in axis formation in the diploblastic metazoan Hydra. *Nature* **407**, 186–189 (2000).
24. U. Technau *et al.*, Parameters of self-organization in Hydra aggregates. *Proc. Natl. Acad. Sci. U.S.A.* **97**, 12127–12131 (2000).
25. M. C. Vogg, B. Galliot, C. D. Tsiairis, Model systems for regeneration: *Hydra*. *Development* **146**, dev177212 (2019).
26. Y. Nakamura, C. D. Tsiairis, S. Özbek, T. W. Holstein, Autoregulatory and repressive inputs localize Hydra Wnt3 to the head organizer. *Proc. Natl. Acad. Sci. U.S.A.* **108**, 9137–9142 (2011).
27. T. Lengfeld *et al.*, Multiple Wnts are involved in Hydra organizer formation and regeneration. *Dev. Biol.* **330**, 186–199 (2009).
28. M. Broun, L. Gee, B. Reinhardt, H. R. Bode, Formation of the head organizer in hydra involves the canonical Wnt pathway. *Development* **132**, 2907–2916 (2005).
29. S. Chera *et al.*, Apoptotic cells provide an unexpected source of Wnt3 signaling to drive hydra head regeneration. *Dev. Cell* **17**, 279–289 (2009).
30. R. Wang, R. E. Steele, E. S. Collins, Wnt signaling determines body axis polarity in regenerating Hydra tissue fragments. *Dev. Biol.* **467**, 88–94 (2020).
31. J. F. Cazet, A. Cho, C. E. Juliano, Generic injuries are sufficient to induce ectopic Wnt organizers in *Hydra*. *eLife* **10**, e60562 (2021).
32. S. Gufler *et al.*, β-Catenin acts in a position-independent regeneration response in the simple eumetazoan Hydra. *Dev. Biol.* **433**, 310–323 (2018).
33. C. Guder *et al.*, An ancient Wnt-Dickkopf antagonism in Hydra. *Development* **133**, 901–911 (2006).
34. S. A. Newman, The interaction of the organizing regions in hydra and its possible relation to the role of the cut end in regeneration. *J. Embryol. Exp. Morphol.* **31**, 541–555 (1974).
35. E. Kobatake, T. Sugiyama, Genetic analysis of developmental mechanisms in hydra. XIX. Stimulation of regeneration by injury in the regeneration-deficient mutant strain, reg-16. *Development* **105**, 521–528 (1989).
36. H. Shimizu, T. Sugiyama, Suppression of head regeneration by accelerated wound healing in hydra. *Dev. Biol.* **160**, 504–511 (1993).
37. H. O. Petersen *et al.*, A comprehensive transcriptomic and proteomic analysis of hydra head regeneration. *Mol. Biol. Evol.* **32**, 1928–1947 (2015).
38. G. C. Manuel, R. Reynoso, L. Gee, L. M. Salgado, H. R. Bode, PI3K and ERK 1-2 regulate early stages during head regeneration in hydra. *Dev. Growth Differ.* **48**, 129–138 (2006).
39. Y. Fabila, L. Navarro, T. Fujisawa, H. R. Bode, L. M. Salgado, Selective inhibition of protein kinases blocks the formation of a new axis, the beginning of budding, in Hydra. *Mech. Dev.* **119**, 157–164 (2002).
40. S. Chera, L. Ghila, Y. Wenger, B. Galliot, Injury-induced activation of the MAPK/CREB pathway triggers apoptosis-induced compensatory proliferation in hydra head regeneration. *Dev. Growth Differ.* **53**, 186–201 (2011).
41. F. Arvizu, A. Aguilera, L. M. Salgado, Activities of the protein kinases STK, PI3K, MEK, and ERK are required for the development of the head organizer in Hydra magnipapillata. *Differentiation* **74**, 305–312 (2006).
42. K. Kaloulis, S. Chera, M. Hassel, D. Gauchat, B. Galliot, Reactivation of developmental programs: The cAMP-response element-binding protein pathway is involved in hydra head regeneration. *Proc. Natl. Acad. Sci. U.S.A.* **101**, 2363–2368 (2004).
43. B. Galliot, M. Welschof, O. Schuckert, S. Hoffmeister, H. C. Schaller, The cAMP response element binding protein is involved in hydra regeneration. *Development* **121**, 1205–1216 (1995).
44. Y. Umesono *et al.*, The molecular logic for planarian regeneration along the anterior-posterior axis. *Nature* **500**, 73–76 (2013).
45. M. Almuedo-Castillo *et al.*, JNK controls the onset of mitosis in planarian stem cells and triggers apoptotic cell death required for regeneration and remodeling. *PLoS Genet.* **10**, e1004400 (2014).
46. M. F. Favata *et al.*, Identification of a novel inhibitor of mitogen-activated protein kinase kinase. *J. Biol. Chem.* **273**, 18623–18632 (1998).
47. F. V. Lali, A. E. Hunt, S. J. Turner, B. M. Foxwell, The pyridinyl imidazole inhibitor SB203580 blocks phosphoinositide-dependent protein kinase activity, protein kinase B phosphorylation, and retinoblastoma hyperphosphorylation in interleukin-2-stimulated T cells independently of p38 mitogen-activated protein kinase. *J. Biol. Chem.* **275**, 7395–7402 (2000).
48. B. L. Bennett *et al.*, SP600125, an anthrapyrazolone inhibitor of Jun N-terminal kinase. *Proc. Natl. Acad. Sci. U.S.A.* **98**, 13681–13686 (2001).
49. S. Hoffmeister, H. C. Schaller, A New Biochemical Marker for Foot-Specific Cell-Differentiation in Hydra. *Wilhelm Roux Arch. Dev. Biol.* **194**, 453–461 (1985).
50. M. M. G. Romero, G. McCathie, P. Jankun, H. H. Roehl, Damage-induced reactive oxygen species enable zebrafish tail regeneration by repositioning of Hedgehog expressing cells. *Nat. Commun.* **9**, 4010 (2018).

51. C. Gauron *et al.*, Sustained production of ROS triggers compensatory proliferation and is required for regeneration to proceed. *Sci. Rep.* **3**, 2084 (2013).
52. D. E. Clapham, Calcium signaling. *Cell* **131**, 1047–1058 (2007).
53. S. K. Yoo, C. M. Freisinger, D. C. LeBert, A. Huttenlocher, Early redox, Src family kinase, and calcium signaling integrate wound responses and tissue regeneration in zebrafish. *J. Cell Biol.* **199**, 225–234 (2012).
54. B. A. Marcum, R. D. Campbell, J. Romero, Polarity reversal in nerve-free hydra. *Science* **197**, 771–773 (1977).
55. H. K. MacWilliams, Hydra transplantation phenomena and the mechanism of hydra head regeneration. I. Properties of the head inhibition. *Dev. Biol.* **96**, 217–238 (1983).
56. H. K. MacWilliams, Hydra transplantation phenomena and the mechanism of Hydra head regeneration. II. Properties of the head activation. *Dev. Biol.* **96**, 239–257 (1983).
57. P. M. Bode, H. R. Bode, Formation of pattern in regenerating tissue pieces of hydra attenuata. I. Head-body proportion regulation. *Dev. Biol.* **78**, 484–496 (1980).
58. J. Yue, J. M. López, Understanding MAPK Signaling Pathways in Apoptosis. *Int. J. Mol. Sci.* **21**, 2346 (2020).
59. S. Cagnol, J. C. Chambard, ERK and cell death: Mechanisms of ERK-induced cell death–apoptosis, autophagy and senescence. *FEBS J.* **277**, 2–21 (2010).
60. E. F. Wagner, A. R. Nebreda, Signal integration by JNK and p38 MAPK pathways in cancer development. *Nat. Rev. Cancer* **9**, 537–549 (2009).
61. J. M. Bugter, N. Fenderico, M. M. Maurice, Mutations and mechanisms of WNT pathway tumour suppressors in cancer. *Nat. Rev. Cancer* **21**, 5–21 (2021).
62. K. E. Wiese, R. Nusse, R. van Amerongen, Wnt signalling: Conquering complexity. *Development* **145**, dev165902 (2018).
63. R. Nusse, H. Clevers, Wnt/β-catenin signaling, disease, and emerging therapeutic modalities. *Cell* **169**, 985–999 (2017).
64. M. B. Labus, C. M. Stirk, W. D. Thompson, W. T. Melvin, Expression of Wnt genes in early wound healing. *Wound Repair Regen.* **6**, 58–64 (1998).
65. C. P. Petersen, P. W. Reddien, Smed-betacatenin-1 is required for anteroposterior blastema polarity in planarian regeneration. *Science* **319**, 327–330 (2008).
66. H. Clevers, K. M. Loh, R. Nusse, Stem cell signaling. An integral program for tissue renewal and regeneration: Wnt signaling and stem cell control. *Science* **346**, 1248012 (2014).
67. H. Yokoyama, H. Ogino, C. L. Stoick-Cooper, R. M. Grainger, R. T. Moon, Wnt/beta-catenin signaling has an essential role in the initiation of limb regeneration. *Dev. Biol.* **306**, 170–178 (2007).
68. J. L. Whyte, A. A. Smith, J. A. Helms, Wnt signaling and injury repair. *Cold Spring Harb. Perspect. Biol.* **4**, a008078 (2012).
69. D. Chuderland, R. Seger, Calcium regulates ERK signaling by modulating its protein-protein interactions. *Commun. Integr. Biol.* **1**, 4–5 (2008).
70. S. Katz, R. Boland, G. Santillán, Modulation of ERK 1/2 and p38 MAPK signaling pathways by ATP in osteoblasts: Involvement of mechanical stress-activated calcium influx, PKC and Src activation. *Int. J. Biochem. Cell Biol.* **38**, 2082–2091 (2006).
71. C. L. Farnsworth *et al.*, Calcium activation of Ras mediated by neuronal exchange factor Ras-GRF. *Nature* **376**, 524–527 (1995).
72. C. E. Paulsen, K. S. Carroll, Orchestrating redox signaling networks through regulatory cysteine switches. *ACS Chem. Biol.* **5**, 47–62 (2010).
73. D. Wenemoser, S. W. Lapan, A. W. Wilkinson, G. W. Bell, P. W. Reddien, A molecular wound response program associated with regeneration initiation in planarians. *Genes Dev.* **26**, 988–1002 (2012).
74. S. Owlarn *et al.*, Generic wound signals initiate regeneration in missing-tissue contexts. *Nat. Commun.* **8**, 2282 (2017).
75. P. Nix, N. Hisamoto, K. Matsumoto, M. Bastiani, Axon regeneration requires coordinate activation of p38 and JNK MAPK pathways. *Proc. Natl. Acad. Sci. U.S.A.* **108**, 10738–10743 (2011).
76. P. Santabárbara-Ruiz *et al.*, ROS-induced JNK and p38 signaling is required for unpaired cytokine activation during *Drosophila* regeneration. *PLoS Genet.* **11**, e1005595 (2015).
77. A. Makanae, A. Hirata, Y. Honjo, K. Mitogawa, A. Satoh, Nerve independent limb induction in axolotls. *Dev. Biol.* **381**, 213–226 (2013).
78. M. Suzuki, A. Satoh, H. Ide, K. Tamura, Transgenic *Xenopus* with prx1 limb enhancer reveals crucial contribution of MEK/ERK and PI3K/AKT pathways in blastema formation during limb regeneration. *Dev. Biol.* **304**, 675–686 (2007).
79. M. H. Yun, P. B. Gates, J. P. Brockes, Sustained ERK activation underlies reprogramming in regeneration-competent salamander cells and distinguishes them from their mammalian counterparts. *Stem Cell Reports* **3**, 15–23 (2014).
80. S. E. Chen, B. Jin, Y. P. Li, TNF-alpha regulates myogenesis and muscle regeneration by activating p38 MAPK. *Am. J. Physiol. Cell Physiol.* **292**, C1660–C1671 (2007).
81. J. Liu, A. Lin, Role of JNK activation in apoptosis: A double-edged sword. *Cell Res.* **15**, 36–42 (2005).
82. M. Motamedi *et al.*, Apoptosis in Hydra: Function of HyBcl-2 like 4 and proteins of the transmembrane BAX inhibitor motif (TMBIM) containing family. *Int. J. Dev. Biol.* **63**, 259–270 (2019).
83. L. Zhang *et al.*, Targeted expression of the dominant-negative FGFR4a in the eye using Xrx1A regulatory sequences interferes with normal retinal development. *Development* **130**, 4177–4186 (2003).
84. D. M. Ouwens *et al.*, Growth factors can activate ATF2 via a two-step mechanism: Phosphorylation of Thr71 through the Ras-MEK-ERK pathway and of Thr69 through RalGDS-Src-p38. *EMBO J.* **21**, 3782–3793 (2002).
85. G. Watson, Z. A. Ronai, E. Lau, ATF2, a paradigm of the multifaceted regulation of transcription factors in biology and disease. *Pharmacol. Res.* **119**, 347–357 (2017).
86. X. S. Wang *et al.*, Genome-wide identification, evolution of ATF/CREB family and their expression in *Nile tilapia*. *Comp. Biochem. Physiol. B Biochem. Mol. Biol.* **237**, 110324 (2019).
87. J. Zhou, B. A. Edgar, M. Boutros, ATF3 acts as a rheostat to control JNK signalling during intestinal regeneration. *Nat. Commun.* **8**, 14289 (2017).
88. M. Inoue *et al.*, The stress response gene ATF3 is a direct target of the Wnt/β-catenin pathway and inhibits the invasion and migration of HCT116 human colorectal cancer cells. *PLoS One* **13**, e0194160 (2018).
89. T. Hai, "The ATF transcription factors in cellular adaptive responses" in *Gene Expression and Regulation*, J. Ma, Ed. (Springer, New York, NY, 2006), pp. 329–340.
90. T. Hai, C. D. Wolfgang, D. K. Marsee, A. E. Allen, U. Sivaprasad, ATF3 and stress responses. *Gene Expr.* **7**, 321–335 (1999).
91. K. Jindrich, B. M. Degnan, The diversification of the basic leucine zipper family in eukaryotes correlates with the evolution of multicellularity. *BMC Evol. Biol.* **16**, 28 (2016).
92. O. Voloshanenko *et al.*, β-catenin-independent regulation of Wnt target genes by RoR2 and ATF2/ATF4 in colon cancer cells. *Sci. Rep.* **8**, 3178 (2018).
93. L. Grumolato *et al.*, β-Catenin-independent activation of TCF1/LEF1 in human hematopoietic tumor cells through interaction with ATF2 transcription factors. *PLoS Genet.* **9**, e1003603 (2013).
94. H. Watanabe *et al.*, Nodal signalling determines biradial asymmetry in Hydra. *Nature* **515**, 112–115 (2014).
95. U. Technau, T. W. Holstein, Head formation in Hydra is different at apical and basal levels. *Development* **121**, 1273–1282 (1995).
96. T. Lebedeva *et al.*, Cnidarian-bilaterian comparison reveals the ancestral regulatory logic of the β-catenin dependent axial patterning. *Nat. Commun.* **12**, 4032 (2021).
97. K. A. Gurley, J. C. Rink, A. Sánchez Alvarado, Beta-catenin defines head versus tail identity during planarian regeneration and homeostasis. *Science* **319**, 323–327 (2008).
98. M. Iglesias, J. L. Gomez-Skarmeta, E. Saló, T. Adell, Silencing of Smed-betacatenin1 generates radial-like hypercephalized planarians. *Development* **135**, 1215–1221 (2008).
99. T. W. Holstein, The role of cnidarian developmental biology in unraveling axis formation and Wnt signaling. *Dev. Biol.* **487**, 74–98 (2022).
100. H. Meinhardt, Beta-catenin and axis formation in planarians. *BioEssays* **31**, 5–9 (2009).
101. M. Mercker *et al.*, β-Catenin and canonical Wnts control two separate pattern formation systems in Hydra: Insights from mathematical modelling. *bioRxiv* [Preprint] (2021). https://doi.org/10.1101/2021.02.05.429954 (Accessed 7 February 2021).
102. A. Gierer, H. Meinhardt, A theory of biological pattern formation. *Kybernetik* **12**, 30–39 (1972).
103. L. Gee *et al.*, beta-catenin plays a central role in setting up the head organizer in hydra. *Dev. Biol.* **340**, 116–124 (2010).
104. O. Chara, E. M. Tanaka, L. Brusch, "Chapter ten–Mathematical modeling of regenerative processes" in *Current Topics in Developmental Biology*, B. Galliot, Ed. (Academic Press, 2014), **vol. 108**, pp. 283–317.
105. M. Mercker *et al.*, β-Catenin and canonical Wnts control two separate pattern formation systems in Hydra: Insights from mathematical modelling. *bioRxiv* [Preprint] (2021). https://doi.org/10.1101/2021.02.05.429954 (Accessed 29 October 2021).
106. M. Mercker *et al.*, How Dickkopf molecules and Wnt/β-catenin interplay to self-organise the Hydra body axis. *bioRxiv* [Preprint] (2021). https://doi.org/10.1101/2021.09.13.460125 (Accessed 29 October 2021).
107. C. L. Stoick-Cooper *et al.*, Distinct Wnt signaling pathways have opposing roles in appendage regeneration. *Development* **134**, 479–489 (2007).
108. A. Tursch, N. Bartsch, T. W. Holstein, MAPK signaling links the injury response to Wnt-regulated patterning in *Hydra* regeneration. *bioRxiv* [Preprint] (2020). https://doi.org/10.1101/2020.07.06.189795 (Accessed 6 July 2020).